IEEE Photonics Journal
An IEEE Photonics Society Publication

Open Access

High-Sensitivity Gas Pressure Sensor Based on Fabry–Pérot Interferometer With a Side-Opened Channel in Hollow-Core Photonic Bandgap Fiber

Volume 7, Number 6, December 2015

Jian Tang
Guolu Yin
Changrui Liao
Shen Liu
Zhengyong Li
Xiaoyong Zhong
Qiao Wang
Jing Zhao
Kaiming Yang
Yiping Wang, Senior Member, IEEE

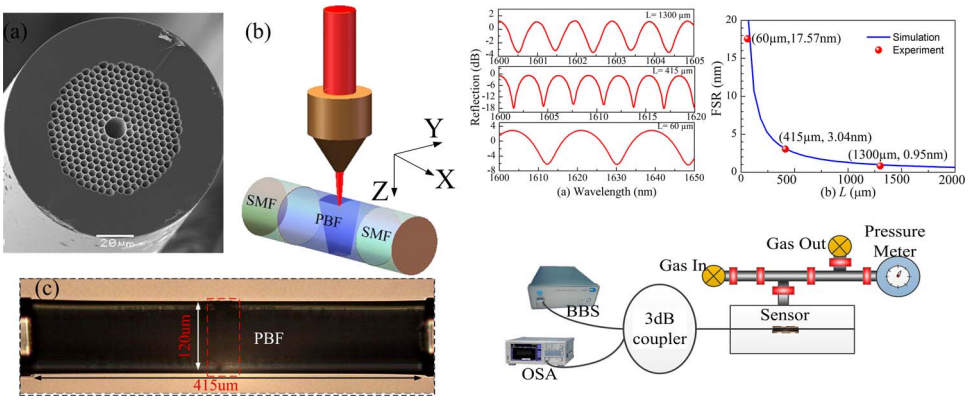

DOI: 10.1109/JPHOT.2015.2489926

High-Sensitivity Gas Pressure Sensor Based on Fabry–Pérot Interferometer With a Side-Opened Channel in Hollow-Core Photonic Bandgap Fiber

Jian Tang, Guolu Yin, Changrui Liao, Shen Liu, Zhengyong Li, Xiaoyong Zhong, Qiao Wang, Jing Zhao, Kaiming Yang, and Yiping Wang, *Senior Member, IEEE*

Key Laboratory of Optoelectronic Devices and Systems of Ministry of Education and Guangdong Province, College of Optoelectronic Engineering, Shenzhen University, Shenzhen 518060, China

DOI: 10.1109/JPHOT.2015.2489926

Manuscript received September 17, 2015; revised October 5, 2015; accepted October 8, 2015. Date of publication October 12, 2015; date of current version October 28, 2015. This work was supported by the National Natural Science Foundation of China under Grant 61425007, Grant 11174064, Grant 61377090, Grant 61575128, Grant 61308027, and Grant 61405128; Guangdong Provincial Department of Science and Technology under Grant 2014A030308007, Grant 2014A030312008, Grant 2014B050504010, Grant 2015B010105007, and Grant 2015A030310243; by the Science and Technology Innovation Commission of Shenzhen/Nanshan under Grant KQCX20120815161444632, Grant ZDSYS20140430164957664, Grant KC2014ZDZJ0008A, and Grant GJHZ20150313093755757; by China Postdoctoral Science Foundation under Grant 2014M552227 and Grant 2015T80913; and by Pearl River Scholar Fellowships. Corresponding author: Y. Wang (e-mail: ypwang@szu.edu.cn).

Abstract: We demonstrate a high-sensitivity gas pressure sensor by use of an in-fiber Fabry–Pérot interferometer (FPI) based on hollow-core photonic bandgap fiber (HC-PBF) with a side-opened channel. The FPI was constructed by splicing a thin piece of HC-PBF between two stander single-mode fibers. Then, a side-opened channel was drilled through the hollow core of the HC-PBF by use of a femtosecond laser. Such an FPI with a side-opened channel greatly enhanced the gas pressure sensitivity up to 4.24 nm/MPa, which is two orders of magnitude higher than that of FPI with an enclosed cavity. In addition, the effects of cavity length on the gas pressure sensing performance were also studied. A shorter cavity gives rise to broader measurement range while offering larger detection limit, and *vice versa*. The structure size is tens of micrometers, which makes it possible to develop an ultracompact high-sensitivity gas pressure sensor.

Index Terms: Fabry–Pérot interferometer, hollow-core photonic bandgap fibers, cavity length, gas pressure sensors.

1. Introduction

Over the past few years, fiber Fabry–Pérot interferometers (FPIs) have been extensively explored for sensing applications due to their distinctive advantages, such as small size, relatively low temperature cross-sensitivity, high resolution, low cost, etc. [1]–[4]. The techniques used for FPIs fabrication include internal film coating [5], fiber Bragg grating [6], laser irradiated points [4], chemical etching [7], focused ion beam techniques [8], and refractive-index mismatch between two fibers in the splicing joint [9]. In 2007, Rao *et al.* proposed a FPI based on hollow-core photonic bandgap fiber (HC-PBF) for the first time [10]. Thus far, it has been widely used for

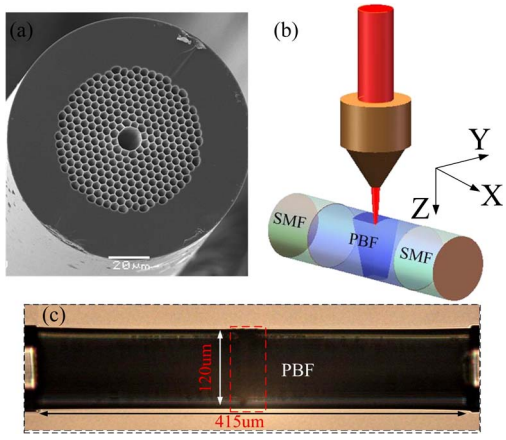

Fig. 1. (a) Cross section of HC-PBF, (b) schematic diagram of FS laser fabrication, and (c) side view of the side-opened drilled FP cavity.

measuring axial strain [11], temperature [12], refractive index, [3] and magnetic [2]. In 2010, Deng *et al.* reported a novel refractive index (RI) sensor based on a FPI by splicing a section of hollow core fiber between a single-mode fiber and a photonic crystal fiber (PCF). The pressure sensitivity can be calculated up to 6.48 nm/MPa. However, the cladding air holes of the PCF are easily destroyed during the splicing process, which may make the external gaseous samples unable to enter the air cavity [13]. In 2012, a FPI based on HC-PBF was proposed to measure N_2 pressure variations with a sensitivity of 3.04 nm/MPa [14], but it has a low extinction ratio, which is not quite suitable in the sensing field. In 2013, L. Jin *et al.* experimentally and theoretically investigated the gas pressure sensitivity characteristics of FPI based on HC-PBF [15]. They theoretical demonstrated that the dominated factor affect the sensitivity is the change of cavity length under applied gas pressure. However, the measured pressure sensitivities is only −0.0234 nm/MPa.

In this paper, we demonstrate a high-sensitivity gas pressure sensor based on a FPI which was formed by splicing a section of HC-PBF between two sections of SMF. A side opened channel was drilled through the hollow core to allow the external gas to fill in the FPI cavity and thus to enhance the interaction between gas and the light signal in the FPI cavity. Experimental results exhibited that such FPI with a side opened channel has a high gas pressure sensitivity up to 4.24 nm/MPa, which is two orders of magnitude higher than the FPI with an enclosed cavity [15]. In addition, the effects of cavity length on the gas pressure sensing performance were also studied in this paper.

2. Fabrication of FPI With a Side Opened Channel

The HC-PBF used in the experiment is HC-1500-02 PBF from Crystal Fiber as shown in Fig. 1(a). The fabrication process of the proposed FPI with a side opened channel includes two main steps. First of all, each end of the HC-PBF with a certain length was spliced to a single mode fiber by use of a commercial fusion splicer (FSM-60) in a manual mode. During splicing the HC-PBF, the end face of the PBF was placed at the region far away from the arc discharge center in order to avoiding collapse the air holes. The fusion parameters such as arc power, arc time and pushing distance were improved to reduce the splice losses and weaken the interference between the fundamental mode and surface modes. An optimized arc power, i.e. stander-60, and an arc time of 400 ms were used in our experiment.

Following the splicing, we drilled a side opened channel through the HC-PBF along the “Z” direction by use of a femtosecond (FS) laser (Spectra-Physics Solstice, 120 fs, 800 nm, 1 KHz, 4 mJ). Fig. 1(b) illustrates the schematic diagram to drill a side opened channel with the help of FS laser. The detailed fabrication processes are depicted as follows: a HC-PBF was mounted on a computer-controlled three-axis translation stage with a resolution of 10 nm. The FS laser

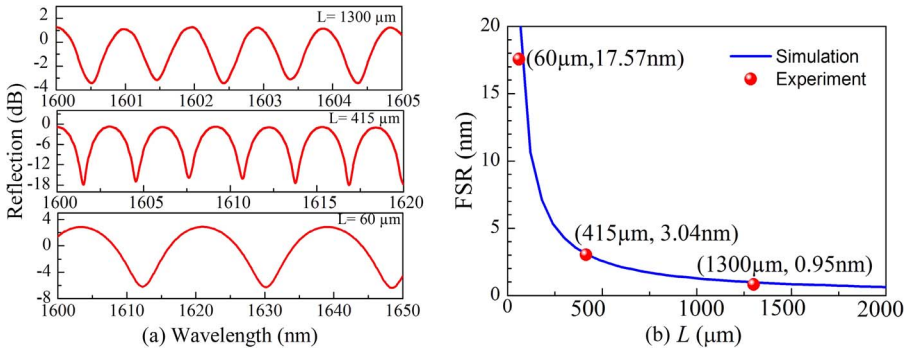

Fig. 2. (a) Measured reflection spectrum (b) measured and calculated FSR of interference fringes of FPIs with lengths of 1300 μm, 415 μm, and 60 μm.

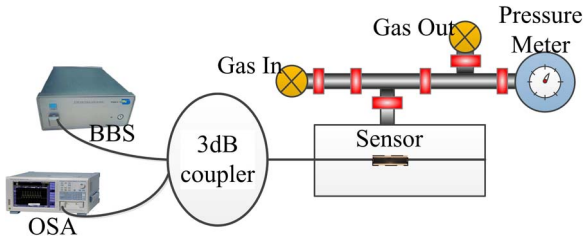

Fig. 3. Experimental setup for gas pressure measurement.

beam was focused onto top surface of the HC-PBF by use of an objective lens with an NA value of 0.25. The focused spot size was $\sim$5 μm and the pulse energy was $\sim$20 mW. First, the focused FS laser beam was scanned with a distance of 20 μm along the "X" axis direction at a speed of 5 μm/s, and then was returned to the jumping-off point. After that, the laser beam was moved toward the "Z" direction with a step of 5 μm to start a new scanning cycle. Such a process was repeated by several times until a side opened channel was drilled in the HC-PBF, the size is about $20 \times 5 \times 120$ μm along the "X", "Y", and "Z" direction, respectively, as shown in Fig. 1(c). After that, a FPI with a side opened channel was completely fabricated.

Repeating the fabrication process as mentioned above, we achieved three samples with different cavity lengths of 1300, 415, and 60 μm. The cavity length was controlled by use of a precise transmission stage and a microscope when cutting the HC-PBF for splicing it with SMF [16]. Fig. 2(a) shows the corresponding reflection spectra of three FPIs in the 1600–1650 nm wavelength range. The reflection spectra of the interferometers exhibit regular interference patterns with a fringe spacing, i.e., free spectral range (FSR). Fig. 2(b) illustrates that the measured FSR is inversely proportional to the cavity length. Meanwhile, we numerically calculated the FSR by the expression $\mathrm{FSR} = \lambda^2/2$ nL, where λ is the wavelength of light, L is the cavity length of the FPI, and $n = 1$ is the refractive index of air. It was found that the measured FSR agrees well with the simulation results.

3. Gas Pressure Experimental Results

We designed an experimental setup to test the gas pressure response of the proposed FPI based on HC-PBF, as shown in Fig. 3. The gas pressure measurements were performed at room temperature. The sensor sample was fixed on a short piece of steel ribbon to keep it straight. Then it was placed into the gas chamber, where a commercial gas pressure generator with a stability of $\pm$0.2 KPa is equipped with a high-precision digital pressure meter (ConST-811) to measure the gas pressure in the chamber. The chamber was fitted with a feed-through and sealed by strong glue to extend the fiber pigtail outside the chamber for real-time measurement.

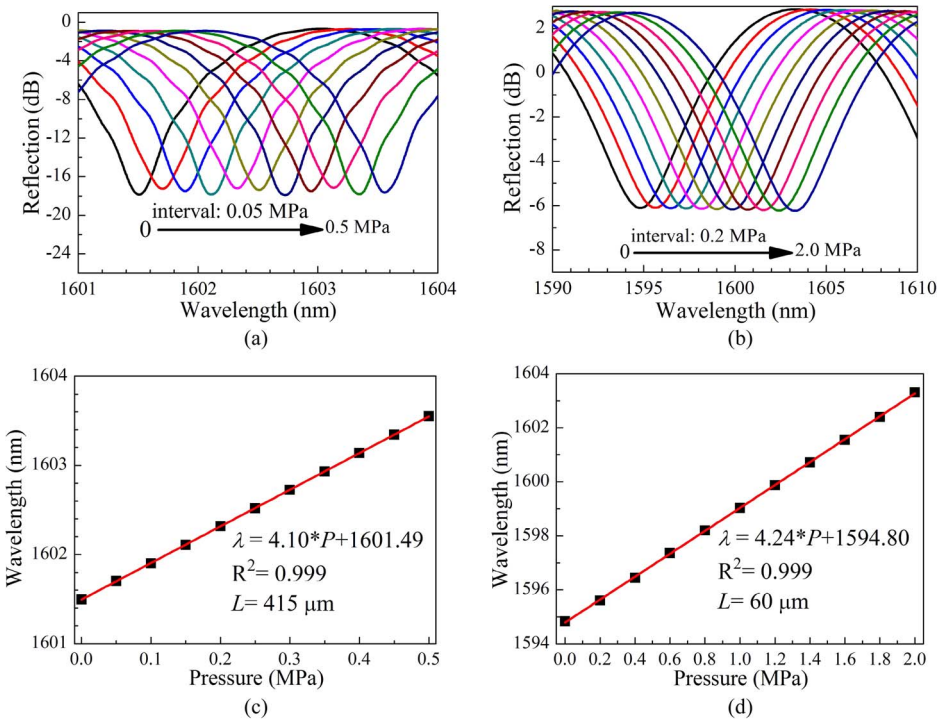

Fig. 4. Reflection spectrum variation of FPI with a cavity length (a) 415 μm, (b) 60 μm and relationship between gas pressure and interference fringe shift of cavity length (c) 415 μm, (d) 60 μm.

A broadband light source (BBS, NKT Photonics SuperK) is connected to one arm of the 3 dB coupler. The output spectrum can be monitored by an optical spectrum analyzer (OSA, YOKOGAWA AQ6370C), which is connected to the other arm of the coupler on the same side. During the gas pressure experiment, each step staying for about ten minutes to observe the stability of the spectrum.

To study the influence of the cavity length on the gas pressure performance, two FPIs with cavity lengths of 415 and 60 μm were used for testing the gas pressure performance. The gas pressure was gradually increased to 0.5 and 2.0 MPa with an interval of 0.05 and 0.2 MPa for two FPIs, respectively. It was found that the interference patterns shift towards longer wavelength with the increase of gas pressure, as shown in Fig. 4(a) and (b). The relationship between dip wavelengths and gas pressure were shown in Fig. 4(c) and (d). It was found that the dip wavelengths shift linearly with sensitivity of 4.10 and 4.24 nm/MPa for the FPI with cavity length of 415 and 60 μm, respectively. A few types of fiber FPI-based gas pressure sensors with different cavity structures were present in Table 1. It can be seen from Table 1 that our current gas pressure exhibits a higher sensitivity of 4.24 nm/MPa, which owes that our proposed sensor with a side opened channel enhanced the interaction between gas and the light signal in the FPI cavity.

Besides the sensitivity, the measurement range and detection limit of the sensor are analyzed as shown in Table 2. When the gas pressure is large enough, the interference dip would move to the initial position of the adjacent dip laying in longer wavelengths. This would leads to the chaos of determining the wavelength shift. Therefore, FSR of the interference spectrum is the maximum distinguishable wavelength shift of the interference dip, and the measurement range is usually defined as the FSR divided by the sensitivity. In our experiment, the FPI with cavity length of 415 and 60 μm has a FSR of 3.04 and 17.57 nm, which provides a measurement range of 0.74 and 4.14 MPa, respectively. The detection limit of a sensor is related to its sensitivity, the resolution of the OSA (0.02 nm in our experiment), the full width at half maximum (FWHM) of the dip or peak, and the signal-to-noise ratio (SNR, $\sim$50 dB in our experiment) of

TABLE 1
Gas pressure sensitivity comparison of a few types of fiber FPI-based gas pressure sensors

Cavity structure	Sensitivity
HC-PBF with enclosed FP cavity [15]	0.0234 nm/MPa
FPI embedded in pressure fittings [18]	0.24 nm/MPa
HC-PBF with an open air-hole FP cavity [14]	3.04 nm/MPa
Fiber-tip air-bubble FPI [19]	1.06 nm/MPa
FPI based on concave well on fiber end [20]	1.53 nm/MPa
FPI with open cavity [21]	2.46 nm/MPa
FPI based on dual capillaries [22]	4.15 nm/MPa
HC-PBF with a side opened channel FPI [our work]	4.24 nm/MPa

TABLE 2
Performance comparison of side opened FPI with different cavity lengths

	Cavity length	
	415 μm	60 μm
Operation wavelength	~1602 nm	~1602 nm
Sensitivity	4.10 nm/MPa	4.24 nm/MPa
FSR	3.04 nm	17.57 nm
Measurement range	0.74 MPa	4.14 MPa
FWHM	0.27 nm	4.27 nm
Detection limit	2.43×10^{-3} MPa	3.69×10^{-2} MPa

the spectrum. The FPI with cavity length of 415 and 60 μm has a FWHM of 0.27 and 4.27 nm, respectively. The detection limit was calculated to be 2.43×10^{-3} and 3.69×10^{-2} according to the formula reported in [17]. Comparing the gas pressure sensing performance in Table 2, we can find that the FPI with shorter cavity length provides large measurement range but also large value of detection limit due to its broader wavelength dip. Consequently, there is a tradeoff between the measurement range and the detection limit for such kind of gas pressure sensor. One should choose proper cavity length according to the demands of the application.

4. Discussion

To study the effects factors of the gas pressure sensitivity, related theoretical derivation were carried out. As mentioned in [15], the gas pressure sensitivity can be expressed by

$$\frac{d\lambda}{dP} = \lambda\left(\frac{1}{L}\frac{dL}{dP} + \frac{1}{n}\frac{dn}{dP}\right). \quad (1)$$

The first term in the bracket depicts the effect of the physical change of the cavity length due to the increment of air pressure. The second term represents the RI variation of the air in the FP cavity under gas pressure.

As we know, the gradually increased gas pressure will induce a longitudinal stain to the FPI and then transfer to the increment of cavity length. The relationship between the cavity length variation and the gas pressure variation can be given by the expression [23]

$$\frac{dL}{dP} = L\frac{1-2\delta}{E} \tag{2}$$

where E is the Young's modulus, δ is the Poisson's ratio, and P is the applied gas pressure. Substituting (2) to (1) and taking $E = 70$ GPa, $\delta = 0.17$ for calculation, the contribution of the cavity-length change to the pressure sensitivity is $\sim$0.015 nm/MPa, which is much smaller than our experimental value of 4.24 nm/MPa. Furthermore, the authors have also demonstrated that the if the holey cladding of the HC-PBF is removed, the sensitivity of -0.021 nm/MPa resulted from cavity length variation only changes by 0.5% in [15]. The reason is that the holey cladding has a large air-filling ratio and small effective Young's modulus, and the longitudinal strain is almost determined by the outer silica cladding [15]. It means that the cavity length variation can be neglected and the gas pressure sensitivity can be simplified expressed as

$$\frac{d\lambda}{dP} = \frac{\lambda}{n}\frac{dn}{dP} \tag{3}$$

where $\mathrm{d}n/\mathrm{d}P$ represents the refractive index variation of air in the FP cavity. At room temperature $(15 \sim 25\ ^\circ\mathrm{C})$, the RI of air is a function of the pressure and temperature [13]

$$n = 1 + \frac{2.8793 \times 10^{-9}}{1 + 0.00367 \times t}P \tag{4}$$

where n, P, t are the RI of air, the pressure (Pa), and the temperature $(^\circ\mathrm{C})$, respectively. dn/dP can be calculated to be 2.63×10^{-3} when the temperature is 25 °C. From Eq. (3) the pressure sensitivity of the FPI can be calculated to be $\sim$4.21 nm/MPa, which is very close to the experimental value of 4.24 nm/MPa. Therefore it demonstrated that the RI variation of the air in the FP cavity plays a dominate role on its gas pressure response.

5. Conclusion

We have experimentally demonstrated a FPI sensor for high-sensitivity gas pressure measurement. The sensor was constructed of a piece of HC-PBF connected to SMF in both ends. A side opened channel was drilled in the HC-PBF to obtain a gas pressure sensitivity of 4.24 nm/MPa, which is in agreement well with the theoretical analysis. In addition, we studied the effects of cavity length on the gas pressure sensing performance and pointed out there is a tradeoff between the measurement range and the detection limit. Such a FPI could be used to develop a promising gas pressure sensor due to its outstanding advantage of being high sensitivity and easy fabrication.

References

[1] Y. Wang *et al.*, "Temperature-insensitive refractive index sensing by use of micro Fabry–Pérot cavity based on simplified hollow-core photonic crystal fiber," *Opt. Lett.*, vol. 38, no. 3, pp. 269–271, Feb. 2013.
[2] Z. Yong, L. Ri-qing, Y. Yu, and W. Qi, "Hollow-core photonic crystal fiber Fabry–Pérot sensor for magnetic field measurement based on magnetic fluid," *Opt. Laser Technol.*, vol. 44, no. 4, pp. 899–902, Jun. 2012.
[3] D. J. J. Hu *et al.*, "Novel miniaturized Fabry–Pérot refractometer based on a simplified hollow-core fiber with a hollow silica sphere Tip," *IEEE Sensors J.*, vol. 12, no. 5, pp. 1239–1245, May 2012.
[4] Y.-J. Rao *et al.*, "Micro Fabry–Pérot interferometers in silica fibers machined by femtosecond laser," *Opt. Exp.*, vol. 15, no. 1, pp. 14123–14128, Oct. 2007.
[5] T. W. Kao and H. F. Taylor, "High-sensitivity intrinsic fiber-optic Fabry–Pérot pressure sensor," *Opt. Lett.*, vol. 21, no. 8, pp. 615–617, Apr. 1996.
[6] S. C. Kaddu, D. J. Booth, D. D. Garchev, and S. F. Collins, "Intrinsic fibre Fabry–Pérot sensors based on co-located Bragg gratings," *Opt. Commun.*, vol. 142, no. 4–6, pp. 189–192, Oct. 1997.

[7] V. R. Machavaram, R. A. Badcock, and G. F. Fernando, "Fabrication of intrinsic fibre Fabry–Pérot sensors in silica fibres using hydrofluoric acid etching," *Sensors Actuators A, Phys.*, vol. 138, no. 1, pp. 248–260, Jul. 2007.
[8] J.-L. Kou, J. Feng, Q.-J. Wang, F. Xu, and Y.-Q. Lu, "Microfiber-probe-based ultrasmall interferometric sensor," *Opt. Lett.*, vol. 35, no. 13, pp. 2308–2310, Jul. 2010.
[9] D. Wu *et al.*, "Intrinsic fiber-optic Fabry–Pérot interferometer based on arc discharge and single-mode fiber," *Appl. Opt.*, vol. 52, no. 12, pp. 2670–2675, Apr. 2013.
[10] Y. J. Rao, T. Zhu, X. C. Yang, and D. W. Duan, "In-line fiber-optic etalon formed by hollow-core photonic crystal fiber," *Opt. Lett.*, vol. 32, no. 18, pp. 2662–2664, Sep. 2007.
[11] S. Qing *et al.*, "Environmentally stable Fabry–Pérot-type strain sensor based on hollow-core photonic bandgap fiber," *IEEE Photon. Technol. Lett.*, vol. 20, no. 4, pp. 237–239, Feb. 2008.
[12] Y. Rao, H. Li, T. Zhu, and M. Deng, "High temperature strain sensor based on in-line Fabry–Pérot interferometer formed by hollow-core photonic crystal fiber," *Chin. J. Lasers*, vol. 36, no. 6, pp. 1484–1488, Jun. 2009.
[13] D. Ming *et al.*, "Refractive index measurement using photonic crystal fiber-based Fabry–Pérot interferometer," *Appl. Opt.*, vol. 49, no. 9, pp. 1593–1598, Mar. 2010.
[14] M. S. Ferreira *et al.*, "Fabry–Pérot cavity based on hollow-core ring photonic crystal fiber for pressure sensing," *IEEE Photon. Technol. Lett.*, vol. 24, no. 23, pp. 2122–2124, Dec. 2012.
[15] J. Long, G. Bai-Ou, and W. Huifeng, "Sensitivity characteristics of Fabry–Pérot pressure sensors based on hollow-core microstructured fibers," *J. Lightwave Technol.*, vol. 31, no. 15, pp. 2526–2532, Aug. 2013.
[16] C. Wu, Z. Liu, A. P. Zhang, B.-O. Guan, and H.-Y. Tam, "In-line open-cavity Fabry–Pérot interferometer formed by C-shaped fiber fortemperature-insensitive refractive index sensing," *Opt. Exp.*, vol. 22, vol. 18, pp. 21757–21766, Sep. 2014.
[17] I. M. White and X. Fan, "On the performance quantification of resonant refractive index sensors," *Opt. Exp.*, vol. 16, no. 2, pp. 1020–1028, Jan. 2008.
[18] G. Z. Xiao, A. Adnet, Z. Y. Zhang, Z. G. Lu, and C. P. Grover, "Fiber-optic Fabry–Pérot interferometric gas-pressure sensors embedded in pressure fittings," *Microw. Opt. Technol. Lett.*, vol. 42, no. 6, pp. 486–489, Sep. 2004.
[19] C. Liao *et al.*, "Sub-micron silica diaphragm-based fiber-tip Fabry–Pérot interferometer for pressure measurement," *Opt. Lett.*, vol. 39, no. 10, pp. 2827–2830, May 2014.
[20] W. Ruohui and Q. Xueguang, "Intrinsic Fabry–Pérot interferometer based on concave well on fiber end," *IEEE Photon. Technol. Lett.*, vol. 26, no. 14, pp. 1430–1433, Jul. 2014.
[21] W. Ruohui and Q. Xueguang, "Gas refractometer based on optical fiber extrinsic Fabry–Pérot interferometer with open cavity," *IEEE Photon. Technol. Lett.*, vol. 27, no. 3, pp. 245–248, Feb. 2015.
[22] B. Xu, C. Wang, D. N. Wang, Y. Liu, and Y. Li, "Fiber-tip gas pressure sensor based on dual capillaries," *Opt. Exp.*, vol. 23, no. 18, pp. 23484–23492, Sep. 2015.
[23] G. B. Hocker, "Fiberoptic sensing of pressure and temperature," *Appl. Opt.*, vol. 18, no. 9, pp. 1445–1448, May 1979.